Stereotactic Localization of Breast Lesions: How It Works and Methods to Improve Accuracy[1]

J. Jeffrey Carr, MD • Paul F. Hemler, PhD • Price W. Halford, MD
Rita I. Freimanis, MD • Robert H. Choplin, MD • Michael Y. M. Chen, MD

A computer simulation of stereotactic breast biopsy was developed that paralleled the geometric configuration of a currently available breast biopsy system. This model was developed to define and improve the targeting of breast lesions with stereotactic biopsy techniques. Lesions must be clearly identified and accurately targeted on both views for successful localization. Nonvisualization of a lesion may result from overlying tissue or from the geometric configuration of the imaging system. Familiarity with the geometric configuration of the biopsy unit, especially the location of the reference point and center of rotation, facilitates understanding of apparent changes in lesion position (parallax shift). Inaccuracy in lesion targeting on one or both views will manifest predominantly as an error in the calculated z value (depth). The magnitude and direction of this error are largely determined by the direction of the targeting error. Compensatory strategies include use of a long-throw core biopsy gun or directional vacuum-assisted biopsy device and additional sampling along the z axis and should be accompanied by critical evaluation of both pre- and postfire images. Understanding geometric considerations as well as how targeting accuracy affects accuracy in lesion localization should lead to greater success in sampling even challenging breast lesions at stereotactic biopsy.

Abbreviations: 3D = three-dimensional, 2D = two-dimensional

Index terms: Biopsies, 00.1261 • Breast, biopsy, 00.1261 • Breast neoplasms, localization, 00.1261 • Computers, simulation • Stereotaxis, 00.1267

RadioGraphics 2001; 21:463–473

[1]From the Department of Radiology, Wake Forest University School of Medicine, Medical Center Blvd, Winston-Salem, NC 27157-1088 (J.J.C., P.F.H., P.W.H., R.I.F., M.Y.M.C.); and the Department of Radiology, Hospital of the University of Pennsylvania, Philadelphia (R.H.C.). Received March 8, 2000; revision requested April 26 and received May 18; accepted May 19. **Address correspondence to** J.J.C. (e-mail: *jcarr@wfubmc.edu*).

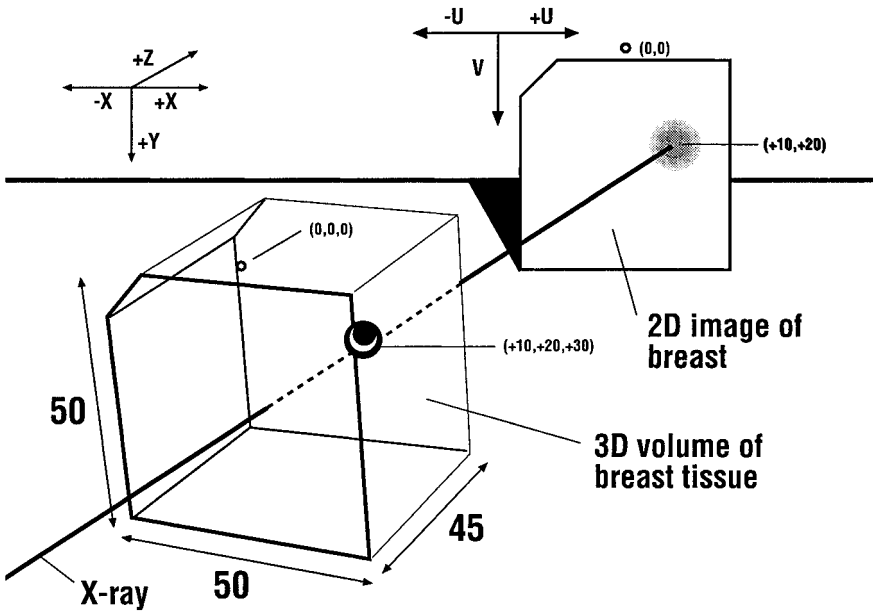

Figure 1. Diagram illustrates the relationship between a 3D object (x, y, and z coordinates) and a 2D image (u, v coordinates).

Introduction

Stereotactic localization of breast lesions has become a common practice in the diagnosis of breast abnormalities. A computer simulation of stereotactic breast biopsy was developed for implementation on a Silicon Graphics (Mountain View, Calif) workstation. This simulation model was used to define and improve the targeting of breast lesions with stereotactic biopsy techniques. It was not intended to reflect the algorithm chosen by a particular vendor but to parallel the geometric configuration of the Lorad StereoGuide digital spot mammography system (Danbury, Conn). Correctional factors, potentially implemented by vendors to optimize performance, were not evaluated.

In this article, we present the basic principles of stereotactic core breast biopsy, explain the reasons for apparent lesion movement or nonvisualization of a lesion, and describe various targeting errors and other geometry-related errors (eg, incorrect x-ray tube positioning, failure to rereference the biopsy needle, patient motion) along with possible compensatory strategies.

Lesion Localization

Stereotactic localization requires a fixed coordinate system. The breast is placed between a compression plate and back breast support to keep the lesion in a fixed position during the procedure. Current biopsy tables have a small imaging field of view, which is determined by the size of the biopsy window in the compression plate and image detector. On the Lorad system, the field of view is 50 × 50 mm. The depth dimension (z) is determined by the thickness of the breast under compression. A lesion within the imaged volume has a unique location that can be described in terms of specific x, y, and z coordinates relative to the point of reference, or origin (0,0,0). On the Lorad system, this reference point is a hole in the compression plate centered above the main biopsy window. The radiograph is a two-dimensional (2D) representation of a three-dimensional (3D) object (the breast), which in the setting of a stereotactic procedure contains a target lesion. The location of the lesion is defined on the 2D image by coordinates on axes designated u and v to help distinguish these coordinates from the x and y coordinates of the 3D object (Fig 1).

Current systems permit angulation about a fixed center of rotation in the x-z plane. An initial (scout) image is obtained with the x-ray beam perpendicular to the compression plate (0° angulation). This scout image is then used to locate and center the lesion in the biopsy window. Once the lesion is properly positioned, a pair of images are obtained after moving the x-ray tube and detector assembly +15° and −15° relative to the 0° position on the scout image. This controlled movement about a known center of rotation creates a pair of images with 30° of separation be-

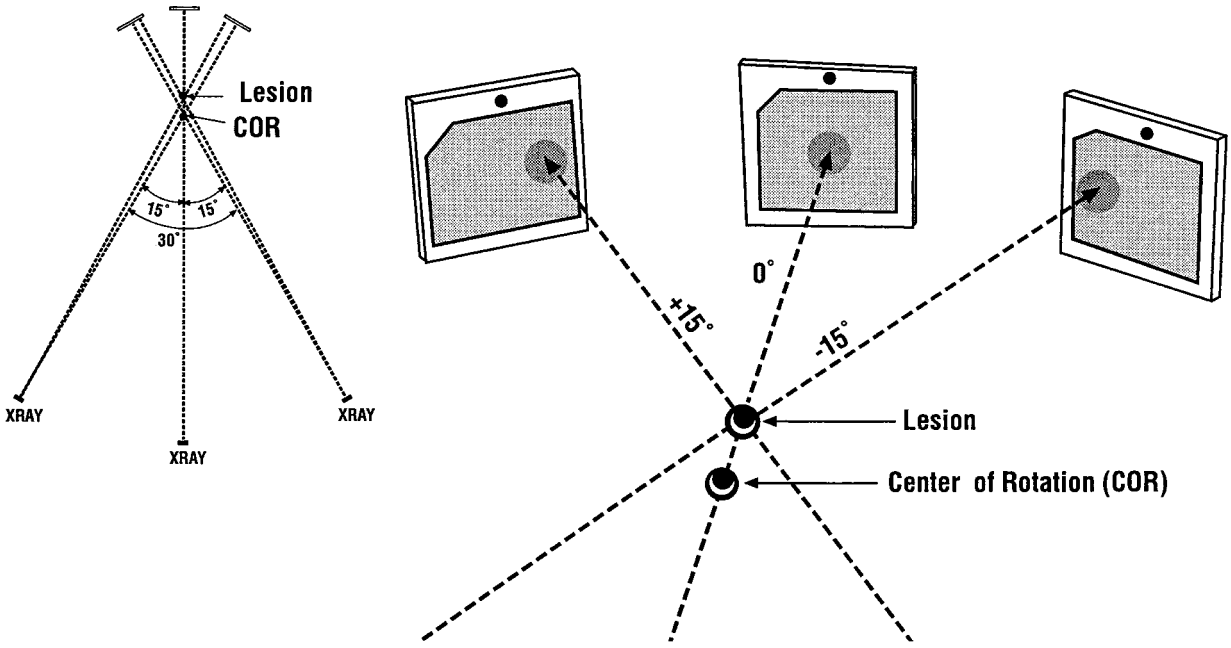

Figure 2. Diagram illustrates the projection of an image on a 2D (u-v) plane at +15°, 0°, and −15° angulation.

tween projections. Basic geometry is used to determine the location of the lesion in the 3D coordinate system with the paired images. Imagine an x ray leaving the tube (a fixed point with respect to the receptor), extending through the center of the lesion, and then intersecting a point on the u-v imaging plane (Fig 2). These two endpoints—the x-ray tube focal spot and the lesion center on the u-v plane—define the location of the x ray in the Cartesian coordinate system. The lesion is known to be located somewhere along the x ray between these two endpoints. An additional projection is needed to determine its exact location and involves rotating the tube and receptor assembly about the center of rotation while the position of the breast (and lesion) remains fixed. The second projection is 30° from the first projection. In practice, a +15° image and a −15° image are produced. Because in theory the lesion has not moved between projections, the two x rays that are responsible for creating the image of the lesion center on the +15° and −15° u-v planes must intersect at the center of the lesion in real space. By equating these two x rays, the x, y, and z coordinates of the lesion can be determined with basic trigonometry.

Apparent Lesion Movement

A reference point is imaged in the stereo views, allowing the u-v imaging plane to be related to the x, y, and z Cartesian coordinates. The apparent movement of the lesion between projections is referred to as parallax shift and is calculated relative to the reference point (1). The terms *parallax shift* and *apparent movement* are used because the breast and lesion do not actually move between projections; however, the projection of the image on the u-v plane does move in a predictable way. This phenomenon is analogous to the use of parallax shift in astronomy. The distance of apparent lesion shift between images can be used to calculate the depth z of the lesion. The location of the center of rotation of the stereotactic biopsy system must be known to understand the significance of the apparent motion of the lesion. If a lesion is located at the center of rotation, the parallax shift is 0; a lesion located farther away from the center of rotation along the z axis will demonstrate an increased apparent motion or parallax shift on the stereo images. It is essential for an operator to know where the reference point and center of rotation are located on the imaging unit.

Major differences exist between the geometric configurations of the Fischer Mammotest system (Denver, Colo) and Lorad system despite their outward similarities (1–4). The two systems define the Cartesian coordinate system differently with respect to the z axis. The z axis is perpendicular to the imaging plane in both systems. However, with the Fischer unit, the location of $z = 0$ is posterior to the breast near the imaging plane, and z increases in value as the object approaches the x-ray source (Fig 3). With the Lorad system, the location of $z = 0$ is anterior to the breast at the reference hole above the biopsy window in the compression plate, and the

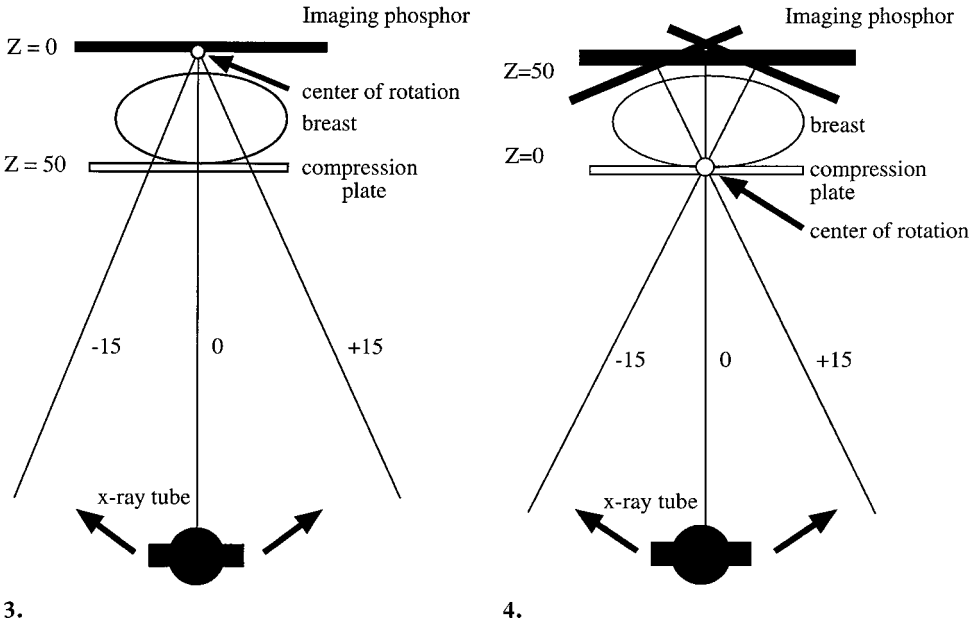

Figures 3, 4. Diagrams illustrate the geometric configuration of the Fischer prone biopsy table **(3)** and the Lorad prone biopsy table **(4)**.

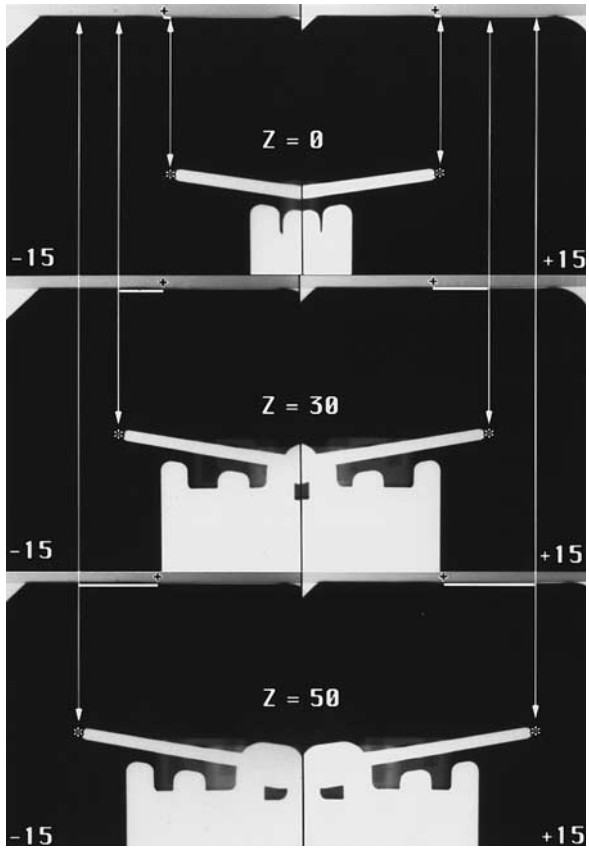

Figure 5. Parallax shift. Three pairs of radiographs obtained at different depths demonstrate parallax shift. The phantom target was a small metal ball at the end of a metal shaft that was positioned at a known location in the imaged volume. Parallax shift was measured by subtracting the x coordinates of the phantom for each pair of views ($x_{+15°} - x_{-15°}$). For Z = 0, Z = 30, and Z = 50, the amount of apparent motion (parallax shift) between images was 0.4, 16.2, and 25.7 mm, respectively. Horizontal line indicates image shift relative to the origin (0,0,0) (+). Note that the sign of the x value must be maintained: On the −15° views (left), the shift is positive for z = 0 but negative for z = 30 and z = 50.

value of z increases as the object approaches the imaging plane (Fig 4). Furthermore, even for the stereo images, the imaging plane on the Fischer unit remains perpendicular to the x ray at 0°, whereas the imaging plane on the Lorad unit rotates with the x-ray source and is always perpendicular to the central x ray. The center of rotation on the Lorad system is adjusted according to the degree of breast compression used.

To demonstrate the effect of lesion depth on the amount of parallax shift, a test object was placed at different depths on the Lorad system. The x and y coordinates were held constant while z was increased from 0 to 50 mm. The apparent motion of the test object relative to the midline of each image was measured (Fig 5) and the results plotted on a graph, which demonstrated a linear relation between lesion depth and parallax shift (Fig 6). The parallax shift seen on the Fischer unit is also plotted on the graph. Note how apparent motion changes inversely to changes in z on the Lorad system.

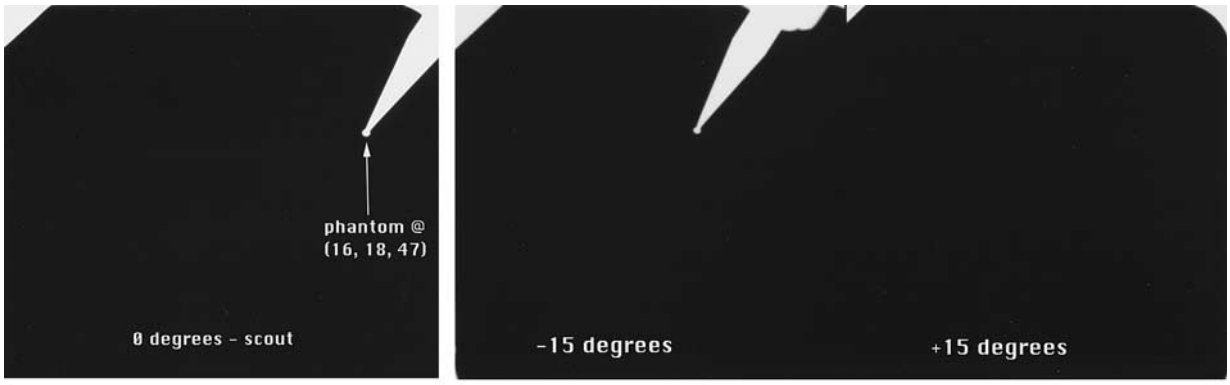

7. 8.

Figures 7, 8. **(7)** Scout radiograph (0° angulation) shows a phantom target at (16,18,47), a point that is 47 mm deep (+z) and 16 mm to the right of midline (+x). **(8)** Stereo radiographs demonstrate the phantom target shown in Figure 7. The target is seen on the −15° image but not on the +15° image.

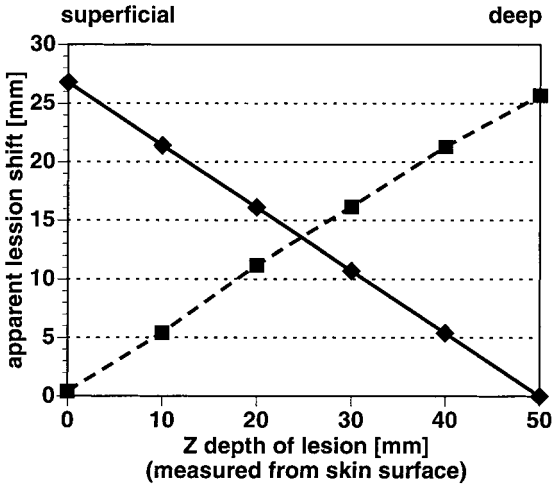

Figure 6. Graph illustrates the relationship between parallax shift (as measured on +15° and −15° images) and depth z (cf Fig 5). With the Fischer system (solid line), parallax shift increases as a lesion is located more superficially. With the Lorad system (dashed line), parallax shift increases with increasing lesion depth. This difference results from the different placement of the center of rotation on the two units.

This difference between the Fischer and Lorad systems is a direct result of the placement of the center of rotation on the two units. On the Lorad unit, the reference point and center of rotation are located anterior to the breast at the compression plate. With this geometric configuration, as lesion depth increases, the amount of apparent lesion motion between the two stereo images (parallax shift) also increases. On the Fischer unit, the center of rotation is located behind the breast near the imaging plane (2). As a result, parallax shift increases when the lesion is closer to the compression plate (ie, more superficial) (Fig 6).

Nonvisualization of the Lesion

With some procedures, the target lesion can be identified on the scout image (0° angulation) but is seen on only one of the stereo images (Figs 7, 8). Failure to identify the lesion on both stereo images prevents localization (5). Although the lesion may be obscured by other tissue, another possibility is that the lesion is not imaged because of the geometric configuration of the imaging system.

The position of the breast and lesion should remain fixed during the study. Figure 9 demonstrates the geometric configuration of a scout image of two lesions (0° angulation). It is essential that the target lesion be centered on the scout image. When the x-ray tube is angled +15° and −15° to create the two stereo images, certain portions of the breast are no longer visualized. In addition, breast tissue not seen on the scout image is seen on the two angulated views (Figs 10, 11).

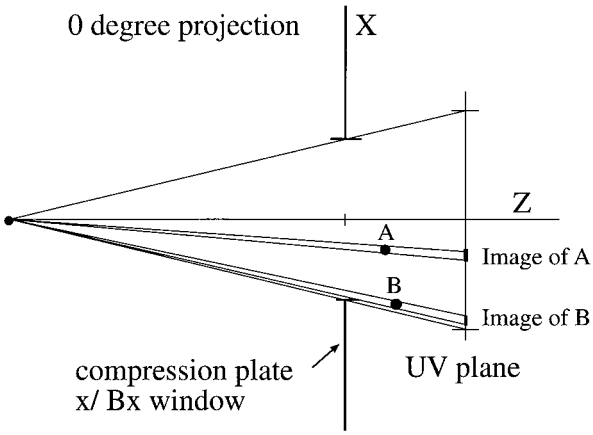

9.

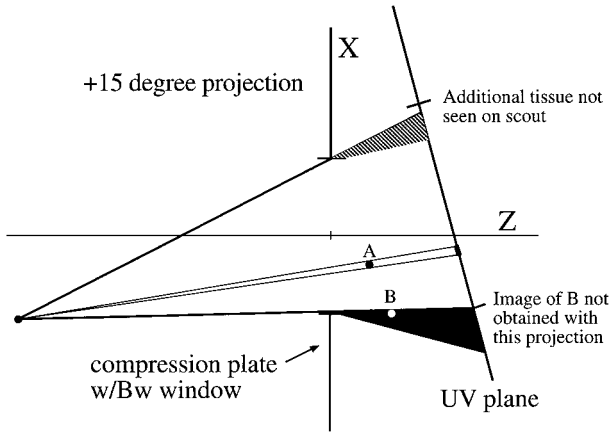

10.

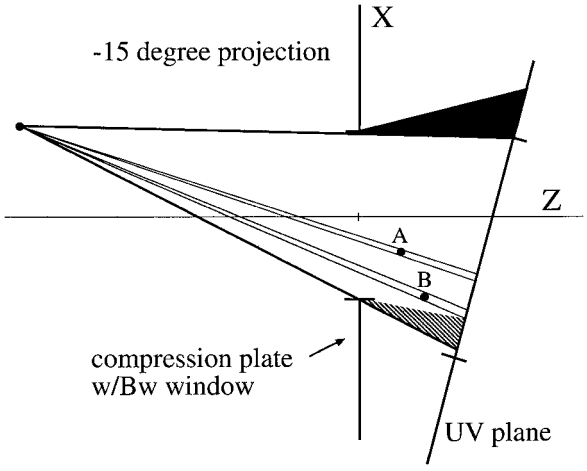

11.

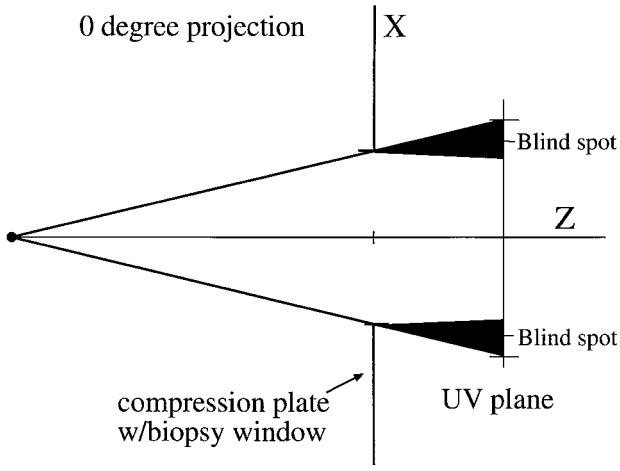

12.

Figures 9–12. **(9)** Diagram shows the location of two objects (*A* and *B*) and their projected images on the u-v plane on a scout image (0° angulation). **(10)** Diagram shows the location of *A* and *B* and their projected images on the u-v plane on an image obtained at +15° angulation. Black triangle indicates a blind spot, which includes object *B*. Hatched triangle indicates breast tissue seen on this image but not on the scout image. **(11)** Diagram shows the location of *A* and *B* and their projected images on the u-v plane on an image obtained at −15° angulation. Black triangle indicates a blind spot, hatched triangle indicates breast tissue seen on this image but not on the scout image. **(12)** Diagram shows blind spots on a scout image obtained with the Lorad system (black triangles). Because lesions located in these blind spots will not be seen on the corresponding +15° and −15° stereo images, localization will not be possible.

The center of rotation and the size of the biopsy window and corresponding imaging plane largely determine the size and location of blind spots. With the Lorad system, the potential blind spots are along the periphery of the biopsy window and enlarge with increasing depth (Fig 12). If a lesion must be positioned peripheral to the biopsy window, the deeper the lesion (+z), the more likely it will "disappear" on one of the stereo images.

To avoid this problem, the lesion should be centered within the imaging field of view on the scout image and the peripheral areas avoided (Fig 12). It is particularly important that the lesion be centered relative to the x (horizontal) axis because the y (vertical) axis remains constant on the stereo images. The lesion should be placed as close as possible to the compression plate (entrance site), a procedure that also decreases the length of the needle track and provides more breast tissue posterior to the lesion. The Fischer system offers the option of using the scout image as a substitute for one of the stereo images (2). This option may allow localization of a lesion seen on only one stereo image because of its location. Use of the scout image reduces the angle between the two projections from 30° to 15°. This decreased angle requires greater accuracy in targeting and is prone to cause slightly larger errors in lesion localization. As the angle between projections increases

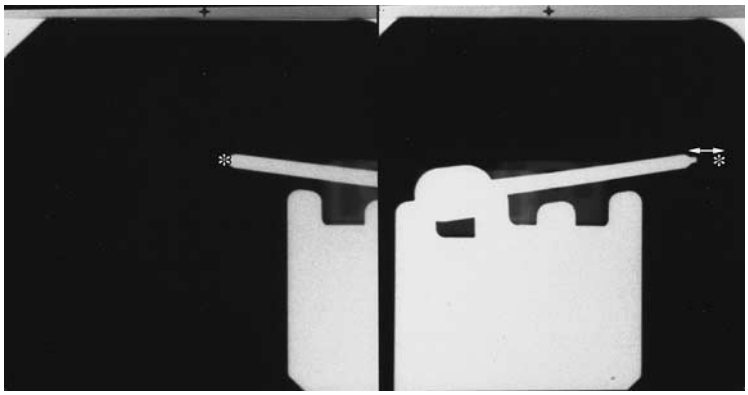

Figure 13. Stereo radiographs show a targeting error (bias) of 3 mm along the x axis on the +15° image (horizontal line) with no error on the −15° image.

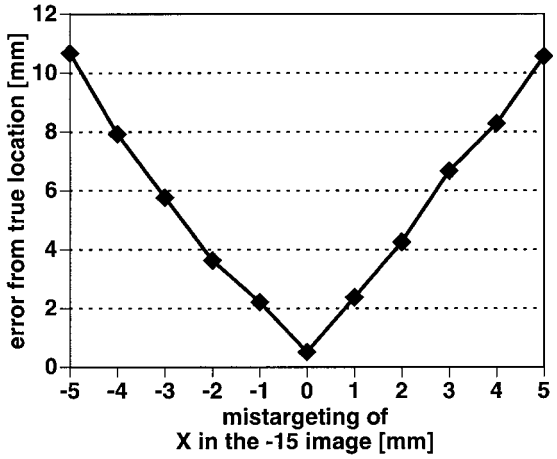

Figure 14. Line graph illustrates the discrepancy between true and calculated location with a targeting error of −5 to +5 mm in the x coordinate on the −15° image. The graph assumes accurate targeting on the +15° image and with respect to y.

(ie, exceeds 30°), the area not visible on the respective stereo images also increases.

Targeting Errors

Stereotactic localization requires that the lesion be seen and accurately targeted on the two paired images. Bias and precision are components of system accuracy. An example of bias is improper referencing ("zeroing") of the needle tip, a procedure in which the tip is assigned specific coordinates in the system used for biopsy. If the tip of the needle is positioned at z = 5 rather than z = 0, a bias of 5 mm is present; the true location of the needle will be +5 mm from the expected location. Precision represents the repeatability of a measurement (ie, the degree to which the same value can be obtained with multiple measurements). A quality control procedure might consist of obtaining multiple images of a phantom target and determining the difference (error) between the true and calculated locations. A mean error that remains constant with a standard deviation that increases suggests a loss of precision. To determine how uncertainty or imprecision in the targeting of lesions affects the calculated location, we placed targets at known locations and then deliberately mistargeted the "lesions" by known amounts on one or both stereo views. Because the y coordinate is held constant for both views, tar-geting error in the vertical dimension was not varied experimentally.

For the +15° view, we mistargeted the lesion by creating a bias of 1–5 mm in both directions (positive and negative) along the x axis. The distance (in millimeters) between the calculated and true locations of the lesion was then determined. Figure 13 demonstrates a targeting error (bias) of 3 mm on the +15° view and accurate targeting on the −15° view.

The error in calculated phantom target location was determined for both the +15° and −15° images for 1-mm increments of mistargeting of the x coordinate. The resulting discrepancy between the true and calculated locations was determined by measuring the straight-line distance between the two points. Figure 14 illustrates the observed error in localization due to mistargeting on the −15° image only. Figure 15 illustrates the error in localization due to mistargeting on either the +15° or −15° image.

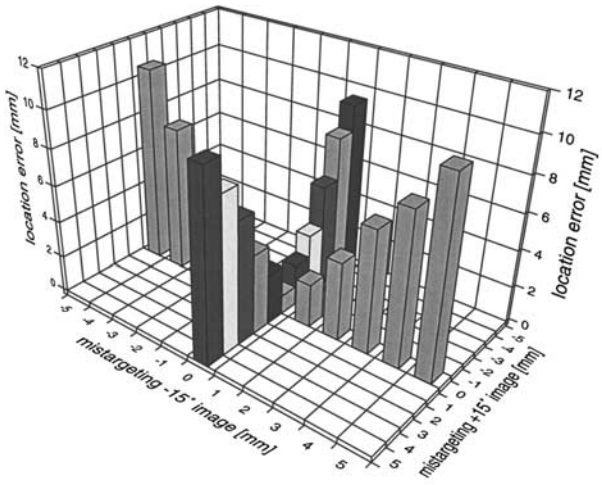

15.

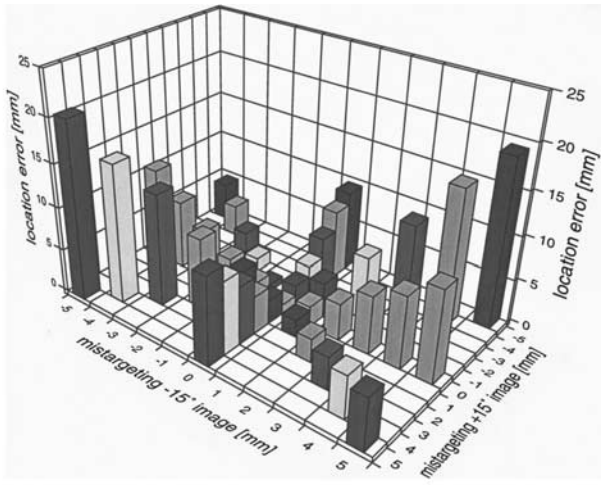

16.

Figures 15, 16. **(15)** Three-dimensional bar graph illustrates localization error (in millimeters) with targeting errors in x on one stereo image and accurate x targeting on the other image. The x and y axes represent the amount of mistargeting, and the height of the column represents the error in localization (ie, the straight-line distance between the true and calculated locations). Note the expected symmetry about "zero error" and between the axes of the two projections. **(16)** Three-dimensional bar graph illustrates localization error (in millimeters) with targeting errors in x on one or both stereo images. Note that opposite targeting errors of −5 and +5 mm on the +15° and −15° stereo views, respectively, result in a 20.5-mm error in localization, whereas error made in the same direction (+5 and +5 mm) produces a difference between the true and calculated locations of only 5.9 mm.

We further evaluated how mistargeting on both views would affect localization. This mistargeting could involve error to the right (+x) on both views, to the left (−x) on both views, or to the right on one view and to the left on the other. The 3D bar graph in Figure 16 illustrates the experimental error in localization observed on the Lorad system with mistargeting on one or both stereo images. Different combinations of targeting errors result in different errors in localization. Furthermore, the direction of targeting error is important. If the bias is in the same direction along the x axis, the apparent shift in lesion location on both views is nearly the same as with accurate targeting and therefore results in the same calculation for lesion depth z; the calculated location will be shifted along the x axis in the corresponding direction. When the targeting errors on the stereo images are in opposite directions along the x axis, the parallax shift will either increase or decrease, creating an error in depth calculation (Figs 16, 17) (1).

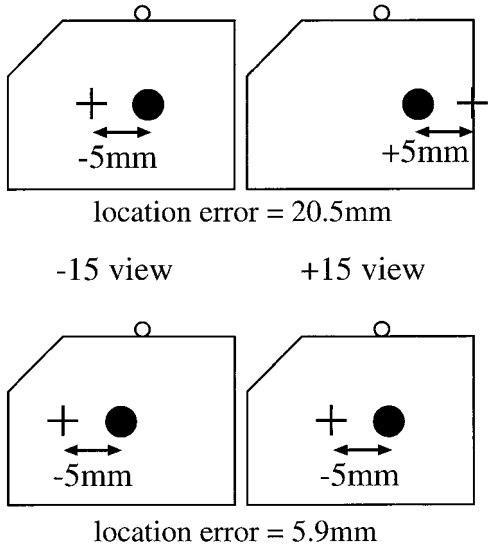

Figure 17. Diagram shows how depth calculation can be markedly altered if the targeting errors are in opposite directions.

The computer simulation allowed us to model the discrepancy between the calculated and true locations for all combinations of targeting errors on +15° and −15° views. The tops of the columns in Figure 18 represent the error surface shown in Figure 19. The theoretic error surface corresponded precisely with the experimentally

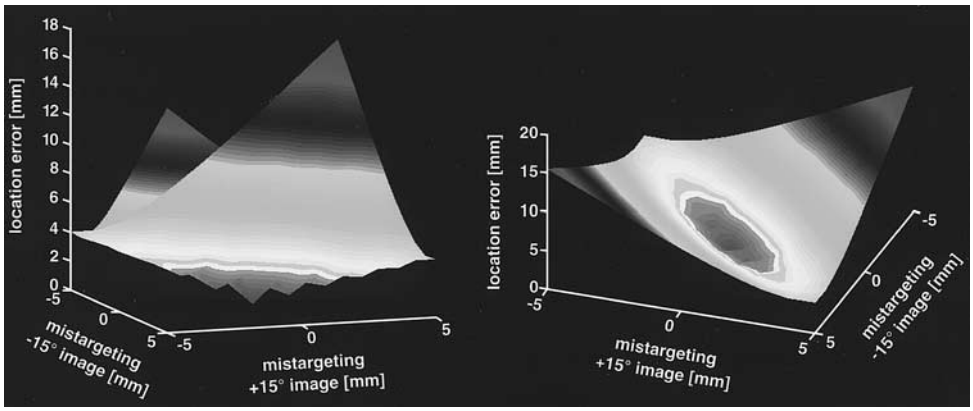

Figure 19. Radiograph illustrates surface display of theoretic error created with all combinations of errors in x targeting on one or both stereo images.

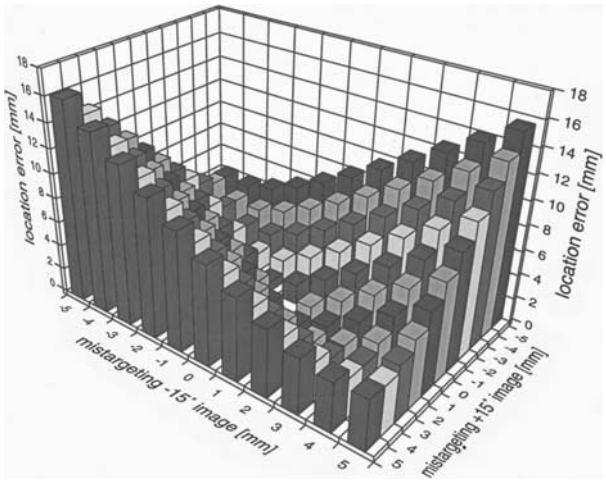

Figure 18. Three-dimensional bar graph illustrates localization error (in millimeters) with targeting errors on both stereo images.

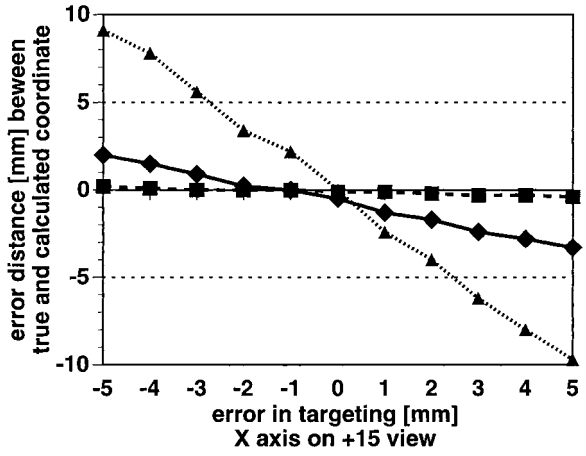

Figure 20. Line graph illustrates the magnitude of error in the x (solid line), y (dashed line), and z (dotted line) coordinates of a phantom whose true location is known. The graph illustrates error on the +15° view only and assumes accurate targeting on the −15° view and with respect to y. Note that when a 3-mm targeting error occurs with respect to x on the +15° view, the difference in y is less than 0.5 mm. The difference in x is less than 3 mm because the x coordinate was accurately targeted on the −15° view. The predominant error involves the value of z and measures over 6 mm in a negative direction.

observed values on the 3D bar graphs in Figures 15 and 16. Figure 20 illustrates the error in each calculated x, y, and z coordinate when compared with the true phantom location for targeting errors ranging from −5 to +5 mm. Note that, depending on the direction in which error is made (ie, to the right or left of the true lesion location), the calculated z value may be either too shallow or too deep.

Targeting errors result in errors in localization for all three coordinates. Most core biopsy procedures use a variety of x and y target coordinates to ensure adequate sampling of the lesion, a sampling technique that may compensate for errors in these two dimensions. However, the depth dimension z is prone to the largest error and is responsible for the majority of errors in localization (Figs 21, 22). The challenge of ensuring adequate sampling, particularly along the z axis, can be at least partially met with use of a long-throw biopsy gun (Fig 23). Current long-throw biopsy guns have a 23-mm throw with a 17-mm sampling notch that should compensate for small targeting errors by encompassing the target, thereby ensuring a successful procedure (5). Use of a directional vacuum-assisted biopsy device can alter the

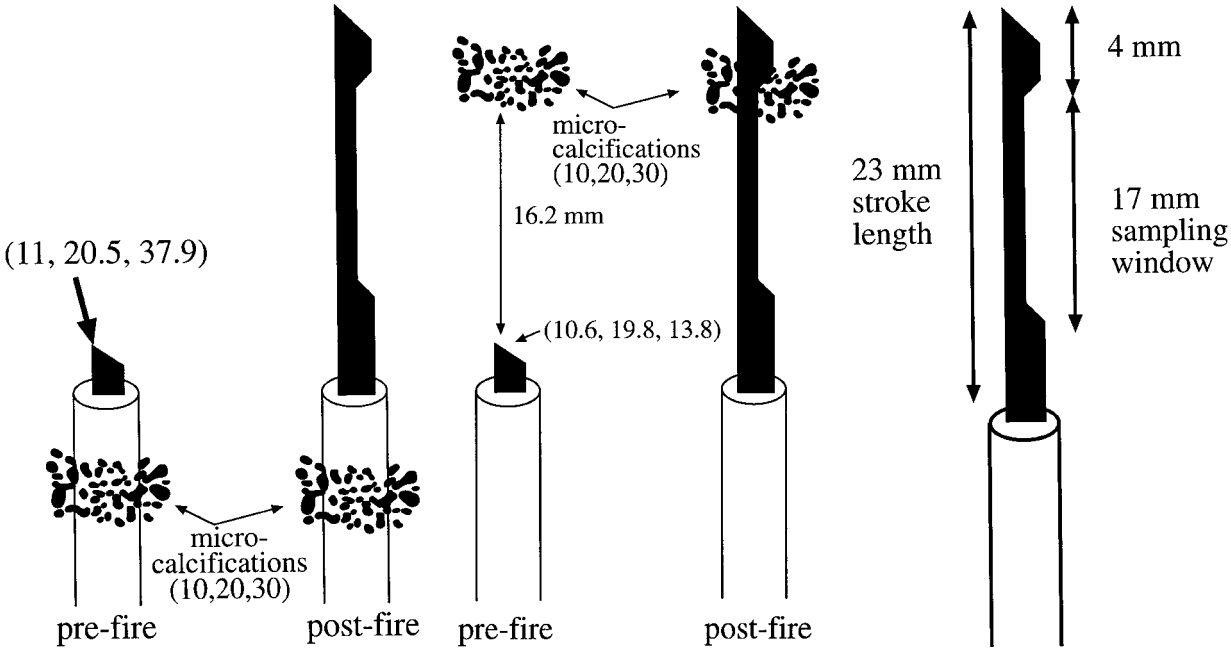

21. 22. 23.

Figures 21–23. **(21)** Diagram shows the results of biopsy when the calculated location is deep to the true location. Targeting errors of +3 and −3 mm have been made on the +15° and −15° views, respectively. The true 3D location of the targeted microcalcifications is (10,20,30). However, the calculated location is (11,20.5,42.9) (ie, 13 mm from the true location). The calculated x and y values are +1 and +0.5 mm, respectively, from the true coordinates. However, the calculated z value is 12.9 mm deep to the true location. If the needle is advanced to a position 5 mm superficial to the calculated location, the tip will be at z = 37.9 prior to firing, or 7.9 mm deep to the true location. Thus, the 17-mm sampling notch would include neither the center of the lesion nor the surrounding area within an 8-mm radius. **(22)** Diagram shows the results of biopsy when the calculated location is shallow to the true location. Targeting errors of −3 and +3 mm have now been made on the +15° and −15° views, respectively, and the true 3D location of the targeted microcalcifications remains (10,20,30). The calculated 3D location is now (10.6,19.8,18.8), or 11.2 mm from the true location. The x and y coordinates are again only slightly in error (0.6 and −0.2 mm, respectively). However, the calculated z value is now 11.2 mm superficial to the true location. If the needle is advanced to a position 5 mm superficial to the calculated location, the tip will be at z = 13.8, or 16.2 mm superficial to the true lesion location. Thus, the 17-mm sampling notch would barely traverse the true lesion location. **(23)** Diagram illustrates a long-throw biopsy gun with a 14-gauge needle.

depth (z value) of the collecting area (bowl) of the probe and yield larger tissue specimens, thereby requiring less stringent targeting. Understanding the potential direction and magnitude of targeting errors is extremely useful in determining the optimal location for sampling with vacuum-assisted biopsy and improves procedure efficiency. Another strategy for improving sampling is to vary z for different biopsy samples. This strategy might include placing the needle tip for core biopsies at various prefire depths. In addition to the routine z = −5, the operator may place the tip 10 mm superficial (z = −15) and 10 mm deep (z = +5) to this location. Obtaining specimens both deep and superficial to the calculated z value is not necessary in all cases but may be valuable if targeting is difficult. Finally, documentation of needle placement with pre- and postfire images is imperative (6). Accuracy in lesion targeting is, of course, preferable to all compensatory strategies.

Other Geometry-related Errors

If the x-ray tube is positioned incorrectly (ie, not exactly at a +15° or −15° angle), the resulting calculations will be incorrect because the images do not have the expected 30° of separation. An error that can cause considerable confusion at first is obtaining images in the wrong sequence. The correct procedure for the Lorad unit is to

obtain the +15° image first, followed by the −15° image. If this order is reversed, the sign of the z value will be reversed and the calculated location will be outside the breast (eg, instead of z = 16, z will be calculated as −16).

A second potential error involves biopsy needle replacement. The needle should always be referenced when placed in the biopsy gun. If a needle becomes contaminated during a procedure and is replaced with a needle of a different length, the system will not recognize this change. If the new needle is not rereferenced, the tip will be at a location different from the calculated location by the difference in length between the two needles.

Patient motion is another potential problem during stereotactic breast biopsy. The breast and lesion are assumed to remain fixed throughout the localization and biopsy procedure. If the breast moves between the time of targeting and the time of positioning the needle, the needle will be located at some position other than the intended target; the actual position will depend on the direction and magnitude of patient motion. The importance of documenting needle position relative to the lesion on prefire images and through the lesion on postfire images cannot be overemphasized. If the prefire images demonstrate a nonoptimal needle trajectory, the lesion should be retargeted and new coordinates calculated, followed by repeat prefire imaging.

Conclusions

Successful stereotactic localization requires that the lesion be clearly identified and accurately targeted on both stereo images. Basic trigonometry is used to determine the x, y, and z coordinates of the lesion center by equating x rays that pass through the lesion on the +15° and −15° views. Familiarity with the geometric configuration of the biopsy unit, especially the location of the reference point and center of rotation, facilitates understanding of apparent changes in lesion position (parallax shift) on the +15° and −15° views. Specifically, this will enable the physician to understand how parallax shift is related to lesion location along the z axis and, perhaps more important, where potential blind spots are located. Thus, the physician will be able to make rapid, accurate decisions regarding repositioning. Inaccuracy in lesion targeting on one or both views will be manifested predominantly as an error in the calculated z value (depth). The magnitude and direction of this error are largely determined by the direction of the targeting error. Compensatory strategies include use of a long-throw core biopsy gun and additional sampling along the z axis and should be accompanied by critical evaluation of both pre- and postfire images. Understanding geometric considerations as well as how targeting accuracy affects accuracy in lesion localization should lead to greater success in sampling even challenging breast lesions at stereotactic biopsy.

References

1. Bolmgren J, Jacobson B, Nordenstrom B. Stereotaxic instrument for needle biopsy of the mamma. AJR Am J Roentgenol 1977; 129:121–125.
2. Burbank F. Stereotactic breast biopsy: its history, its present, and its future. Am Surg 1996; 62:128–150.
3. Lorad. Operators manual. Rev 2. Danbury, Conn: Lorad, 1994; 1–50.
4. Lorad. User's guide. Rev 2. Danbury, Conn: Lorad, 1995; 1–82.
5. Fine RE, Boyd BA. Stereotactic breast biopsy: a practical approach. Am Surg 1996; 62:96–102.
6. Parker SH. Stereotactic large-core breast biopsy. In: Parker SH, Jobe WE, eds. Percutaneous breast biopsy. New York, NY: Raven, 1993; 61–79.